AtFer4 ferritin is a determinant of iron homeostasis in Arabidopsis thaliana heterotrophic cells

Abstract
In plants, the iron storage protein ferritin can be targeted to both chloroplasts and mitochondria. To investigate the role of *Arabidopsis* ATFER4 ferritin in mitochondrial iron trafficking, *atfer4-1* and *atfer4-2* mutant knock-outs for the *AtFer4* gene were grown in heterotrophic suspension cultures. Both mutants showed altered cell size and morphology, reduced viability, higher H2O2 content and reduced O2 consumption rates when compared to wt. Although no reduction in total ferritin or in mitochondrial ferritin was observed in *atfer4* mutants, total iron content increased in *atfer4* cells and in *atfer4* mitochondria. Transcript correlation analysis highlighted a partial inverse relationship between the transcript levels of the mitochondrial ferric reductase oxidase *FRO3*, putatively involved in mitochondrial iron import/export, and *AtFer4*. Consistent with this, *FRO3* transcript levels were higher in *atfer4* cells. We propose that the complex molecular network maintaining Fe cellular homeostasis requires, in *Arabidopsis* heterotrophic cells, a proper balance of the different ferritin isoforms, and that alteration of this equilibrium, such as that occurring in *atfer4* mutants, is responsible for an altered Fe homeostasis resulting in a change of intraorganellar Fe trafficking.

Abbreviations
BPDS4,7-diphenyl-1,10-phenantrolinedisulfonic acidCTABcetyl trimethyl ammonium bromideDAB3,3′-diaminobenzidine tetrahydrochlorideDWdry weightMS mediumMurashige Skoog mediumSHAMsalicylhydroxamic acidFWfresh weightROSReactive Oxygen SpeciesTETris-EDTAT-DNAtransferred DNAWTwild-type

Keywords
*Arabidopsis*Cell deathFerritinIronMitochondria

Introduction
Iron is an essential element for all living organisms: present in the catalytic moiety of many key enzymes (as heme or [Fe-S] cluster) it confers a wide range of redox potentials to them (Guerinot and Yi, 1994). However, when in a free form, Fe is noxious for cells because Fe (III) and Fe (II) catalyze the Fenton reaction, thus contributing to the production of hydroxyl radicals OH▪ and to the consequent damage of macromolecules (Bowler et al., 1992).
Ferritins are proteins that sequester free Fe (II) in a safe, bioavailable form. Ferritin subunits assemble in a cage-like complex with oxidase activity; Fe (II) is oxidized to Fe (III) and deposited as a hydrous ferric oxide mineral core with a variable content of phosphate inside a 24-mer hollow sphere (Arosio et al., 2009). The production of the Fe core requires an oxidant, which can be either O2 or H2O2 and thus using the same reagents as the toxic Fenton reaction (Arosio et al., 2009). Due to these characteristics, ferritins are considered important antioxidants for cells. They are present in all living organisms, except in yeast (Arosio et al., 2009; Briat et al., 2010), where the only putative Fe-storage protein identified thus far is frataxin (Murgia et al., 2009). Interestingly, expression of either human l-ferritin or the human mitochondrial ferritin enhances protection against oxidative stress in frataxin-deficient yeast mutants (Campanella et al., 2004).
In mammalian cells, ferritin localization is cytoplasmic, mitochondrial, nuclear or secretory (Arosio et al., 2009). Cytoplasmic ferritin is expressed in almost every tissue (Mackenzie et al., 2008), whereas the mitochondrial ferritin FtMt, encoded by an atypical intronless gene (Levi et al., 2001), is expressed in highly metabolically active cells (Santambrogio et al., 2007). The role of FtMt as Fe storage and supply seems relevant in mitochondria with intense metabolic activity (Levi and Rovida, 2009), and evidence that the primary function of FtMt involves the control of ROS formation through the regulation of mitochondrial iron availability has been recently presented (Campanella et al., 2009).
Plant ferritins share the same 24-mer quaternary structure as their animal counterparts (Briat et al., 2010). *Arabidopsis* plants possess four ferritin genes, *AtFer1-4*. The recent characterization of a triple *atfer1,3,4* mutant showed that, at least in *Arabidopsis*, the physiological role of ferritin is to protect cells against oxidative stress (Ravet et al., 2009). Though plant ferritins are localized mostly

in chloroplasts (Briat et al., 2010), they can also be found in mitochondria (Zancani et al., 2004; Tarantino et al., 2010), which are organelles with high iron demand, therefore necessitating strict regulation of Fe uptake, storage and availability, as it is true for their animal counterparts (Campanella et al., 2004). Fe efflux from plant mitochondria possibly occurs through the ABC-like transporter STA1 (Kushnir et al., 2001; Briat et al., 2007). Little is known about the mechanisms of iron transport into plant mitochondria (Jeong and Guerinot, 2009), but it has recently been shown that two *Arabidopsis* members of the FRO (ferric reductase oxidase) family are putatively localized in mitochondria, i.e. the FRO3, which is induced upon Fe deficiency and FRO8, which is not regulated by Fe availability (Mukherjee et al., 2006; Jeong and Connolly, 2009). The topological orientation of the encoded proteins is not clear, making it uncertain whether they are involved in Fe import or efflux from mitochondria.

The physiological relevance of ferritin inside plant mitochondria is still unresolved. Indeed, *atfer4-1* and *atfer4-2 Arabidopsis* KO for the mitochondrial ATFER4 isoform (Ravet et al., 2009; Tarantino et al., 2010) do not show any symptoms of higher sensitivity to abiotic stresses, not even to Fe excess (Tarantino et al., 2010). However, it is possible that in photosynthetic tissues, homeostasis of mitochondrial Fe is not as crucial as in non-photosynthetic tissues.

To investigate, in detail, the physiological relevance of *AtFer4* ferritin in non-photosynthetic tissues, *atfer4-1* and *atfer4-2* mutants were grown as suspension cell cultures under heterotrophic conditions, in which proplastids do not differentiate into mature, photosynthetically active plastids, so that mitochondria are the only organelles competent for energy supply.

Materials and methods

Cells growth conditions

Arabidopsis atfer4-1, *atfer4-2* and wt (Col ecotype) suspension cultured cells were established from sterilized *Arabidopsis* seeds, which were laid onto Petri dishes containing the following growth medium: 0.22% Murashige Skoog (MS) medium (Duchefa, Netherlands); 1% sucrose; 10 µM 2,4 D; 3 µM kinetin; 1% Plant agar (Duchefa, Netherlands); and 0.5% MS vitamin solution 1000× (Sigma, cod. M3900). Plates were kept in the dark until the appearance of the first calli (around 4 weeks). Calli were then transferred onto the following liquid medium: 3% sucrose; 0.43% MS salt mixture (Sigma cod. M5524) (final Fe content of MS medium is 100 µM FeSO4); 3 mM MES pH 5.8; 0.2 mg/L 2,4 D; 0.05 mg/L kinetin; 1× MS vitamin solution 1000× (Sigma, cod. M3900); 10 mg/L vitamin B1; 0.5 mg/L vitamin H; 0.5 mg/L folic acid. Cells were grown under constant shaking. Cell lines were propagated by transferring 1 mL compact cell volume into 100 mL growth medium every 7 d.

The growth conditions described above was the control; the condition in which cells were exposed to Fe excess, corresponding to 18 h treatment with 500 µM Fe (III)-citrate before collection (Murgia et al., 2002), is indicated as '+Fe'. Experiments were performed, unless otherwise specified, with 7 d cell cultures. Cell suspensions were filtrated through a 25 µm nylon cloth with suction.

Cell viability

Seven d cell cultures were used for inoculating, for each time-point, 2 different flasks with 1 mL compact cell volume each. For each time point and for each cell line, contents of two flasks were rapidly mixed and filtered through a 25 µm nylon cloth with suction. Cells were then weighed and cell samples (300 mg FW) were put in Transwell cell culture chambers with permeable supports (24 mm diameter, 8 µm filter pore size, Corning Costar Corp., Corning, NY, USA) containing 5 mL fresh MS medium and kept under gentle shaking (80 rpm).

Each well was supplemented with 25 µL Evans Blue dye stock solution (15.6 mM in H2O) and cells were stained for 10 min under gentle shaking at room temperature. To remove dye not entered into the cells, filters were first allowed to dry onto filter paper and then put back into the wells and washed with fresh water at least 8 times. Cells were then transferred into 2 mL vials with screw caps containing 500 µL extraction buffer (50% methanol, 1% SDS) and glass beads were added to the vials; cells were disrupted with the Hybaid Ribolyser (Celbio, Italy). Vials were centrifuged 1 min at the maximum speed in a bench centrifuge and supernatants were collected. Dye extraction from the pellets was repeated two more times. The collected supernatants were then

centrifuged one more time for 1 min at the maximum speed; 50 µL supernatant were diluted with 950 µL extraction buffer and absorbance at 600 nm was quantified on a Jasco V-530 spectrophotometer.
To establish the absorbance of 100% dead cells, aliquots of cells maintained in liquid nitrogen for 10 min were also stained using the procedure described above.
Protein and DNA quantification
Crude protein cell extracts were prepared as described in Murgia et al. (2002). Protein concentration was measured by the Lowry procedure (Sigma Diagnostic Protein Assay Kit) following the manufacturer's instructions.
DNA extraction was performed as follows: 100 mg cells were disrupted with a Hybaid Ribolyser cells disruptor with the help of glass beads, after addition of 600 µL CTAB buffer (3% CTAB, 1.4 M NaCl, 20 mM EDTA, 100 mM Tris HCl, pH 8.0, 0.2% β-mercaptoethanol added shortly before use) in each tube. Samples were incubated 30 min at 60 °C, then 250 µL CHCl3 were added and samples were centrifuged 5 min at 13,000 × *g*. The supernatants were transferred into fresh tubes and, after adding 330 µL isopropanol, they were kept 30 min at -20 °C and then centrifuged 3 min at 6000 × *g*. DNA pellet was washed with 75% ethanol and resuspended in 50 µL TE buffer. DNA was quantified spectrophotometrically at 260 nm.
RT-PCR
Total RNA was extracted from 100 mg cells with Trizol® reagent (Gibco) and RT-PCR amplification reactions were performed by using the DyNAmo cDNA Synthesis Kit (Finnzymes, Finland) following the manufacturer's instructions. cDNA fragments were amplified by diluting 1:20 cDNA templates in nuclease-free water; 1 µL cDNA was used as template for each PCR reaction, with the following primers:
AtFer1for: 5′-TAAGCCACTACTCCCTCACG-3′
AtFer1rev: 5′-TTTGTGAACGTTTAGAAGCTTCTC-3′ (574 pb fragment size, 63 °C anneal. temp., 2 mM MgSO4).
AtFer2 for: 5′-GGAACGAACACGAAGTCGTTAACCGG-3′
AtFer2rev: 5′-CTCGTTCTTCAAGACTCGAATCGTT-3′ (264 pb fragment size, 55 °C anneal. temp., 2 mM MgSO4).
AtFer4for: 5′-TTTCCATGGCGTGAAGAAGG-3′
AtFer4revbis: 5′-ATGTTCAAACTCTGAAAGAGGC-3′ (472 bp fragment size, 52 °C annealing temp., 20 ng total RNA, 1.5 mM MgSO4).
Specificity of primers for the *AtFer4* gene was verified at http://www.arabidopsis.org/Blast/index.jsp by BLASTN search against the collection of TAIR9 genes.
FRO3for: 5′-TTCAATAGCAGTAAGGTTAGG-3′
FRO3rev: 5′-AAGCTCGACAGTTTCACAAGG-3′ (526 bp fragment size, 60 °C anneal. temp., 2.5 mM MgSO4).
FRO7 for: 5′-TTCGAGCATGCTACAAGATACC-3′
FRO7 rev: 5′-TTACGGTGTAGGATATCGC-3′ (806 bp fragment size, 60 °C annealing temp., 60 ng total RNA, 2.5 MgSO4).
FRO8 for: 5′-AAGTACTATAGAGTTGCTACAAGG-3′
FRO8rev: 5′-GATTGGCGGAAAGAATGCAGC-3′ (511 pb fragment size, 60 °C anneal. temp., 2.5 MgSO4).
STA1for: 5′-AGCTCTCCGAACAATACGAT-3′
STA1rev: 5′-GCCCTTGTGCTAGCATCATTAT-5′ (349 pb fragment size, 63 °C anneal. temp., 1.5 MgSO4).
Amplification of AtFer3 *and Tub4* was performed as described in Tarantino et al. (2003).
Protein gel blot analysis
Protein extracts were prepared as described in Murgia et al. (2007). Two polyclonal antibodies were used to detect *Arabidopsis* ferritins. The first, called anti-Ferritin here and first described in Murgia et al. (2007), was raised against an antigen oligopeptide corresponding to aa 60–74 in ATFER1 sequence with high homology (63–68% conserved aa residues) to the other ferritin

isoforms ATFER2, ATFER3, ATFER4. The second, called anti-ATFER1 here and first described in Dellagi et al. (2005), was raised against ATFER1 full protein; anti-Ferritin antibody was used at 1:2000 dilution and anti-ATFER1 antibody at 1:10,000 dilution.
As a secondary antibody, a goat-antirabbit conjugated with HRP (Amersham Biosciences) was used at 1:25,000 dilution for the anti-Ferritin antibody and at 1:5000 dilution for the anti-ATFER1 antibody. Signals were detected with the kit SuperSignal® West Pico (Pierce-Celbio Srl, Italia) and a stripping procedure was performed with the Restore Western Blot Stripping Reagent (Pierce-Celbio Srl, Italia), following the manufacturer's instructions. Gel blot analysis of NAD9 and AOX mitochondrial proteins was performed as in Vigani et al. (2009). Images were acquired by the AlphaEaseFC Imaging System (Alpha Innotech) with the AlphaEaseFC software.
Mitochondria purification of suspension cultured cells
Isolation of mitochondria from heterotrophic *Arabidopsis* cell suspension cultures was performed by following, step by step, the protocol described in Sweetlove et al. (2006). Determination of mitochondrial integrity was performed with the cytochrome-c oxidase assay also described in Sweetlove et al. (2006).
Total iron content in mitochondria and whole cells
For mitochondria, samples were mineralized in Pirex tubes previously washed with 2N HCl and rinsed with ddH2O. 50 µL 65% HNO3 and 50 µL 95–98% H2SO4 were added in tubes, each containing 330 µg mitochondrial total proteins. Samples were mineralized 5 h in a thermoblock at 200 °C (or overnight at 120 °C) under a chemical hood and, after cooling down, if not transparent, 50 µL HClO4 were added. The following reagents were then added in order, with vortexing between each addition: 200 µL 5.5 M Na-acetate, 400 µL H2O, 50 µL 10% (v/v) thioglycolic acid freshly prepared and 50 µL 5% (w/v) BPDS freshly prepared. After 30 min samples become purple; if not, 50 µL 10 N NaOH were added and samples were incubated 30 min, Sample absorbance at 540 nm was determined. For the calibration curve, 0, 70, 125, 250, 500 and 1000 ng FeCl3 were prepared from a 1 mg/mL FeCl3 stock solution (Carlo Erba, Italy, n. 497511) and quantified as indicated above. For whole cells, samples of 100 mg FW were incubated with 200 µL 65% HNO3 and 200 µL 95–98% H2SO4 and then vortexed until the cell suspension clarified; 100 µL aliquots were used for the mineralization, as indicated above.
DAB staining
Cells (one drop) were resuspended in 10 mL growth medium. 10 mL DAB solution were added, samples were incubated overnight in the growth chamber with constant shaking, and cells were then observed under a light microscope. DAB solution (1 mg/mL, pH 5.5) was prepared fresh before use.
O2 consumption rates
Oxygen consumption was measured as described in Tarantino et al. (2010), in a final volume of 1.8 mL culture medium containing 0.1 g filtered cells from a 7 d suspension of cultured cells. For O2 consumption measurements carried out in the presence of KCN, cells were resuspended in non-autoclaved culture medium, since autoclaving of sucrose produces degradation products which are known to react with oxygen in the presence of KCN, as reported in Hsiao and Bornman (1989).
The stock solutions were: 250 mM SHAM in 100% ethanol; 250 mM KCN in water.
Light microscopy and TEM analysis
Cells were fixed with 3% glutaraldehyde for 24 h at 4 °C in growth medium, as indicated in Vazzola et al. (2007), post-fixed with 1% OsO4 for 2 h at 4 °C and then gradually dehydrated, first in a series of ethanol and, finally, in propylene oxide. Infiltration was subsequently performed with a mixture of propylene oxide-resin (Araldite-Epon) in volume proportions of 2:1 for 1 h and 1:1 overnight, respectively. Cells were then embedded 4 h in 100% pure resin and polymerization was performed at 60 °C for 24 h. Sections were made on an Ultracut E microtome (Reichert); semithin sections of 1 µm were collected onto a microscope slide, stained with 1% toluidine blue and observed with a Leica DMRA2 optical microscope (Leica Microsystems). Ultrathin sections of 80 nm, made with a diamond knife (Diatome), were collected on 200 mesh formvar/carbon copper

grids and examined using a EFTEM Leo912ab transmission electron microscope (Zeiss) at 80 kV. Three independent fixation experiments were performed by using, for each, cell samples collected in different weeks. Also, for each fixed sample, several cuts were performed and analyzed. Digital images were acquired using an Esivision CCD-BM/1K system.

Expression correlation analysis

The calculation of the Pearson's correlation coefficients between expression level for every gene pair was performed by using a dataset of 1750 microarray hybridizations as described in Menges et al. (2007, 2008). Calculations were performed on the expression values as such or after logarithmic transformation.

Results

atfer4 cells show no reduction in total ferritin content but an increase in total Fe content

Suspension cultured cells of wt Col and of *atfer4-1* and of *atfer4-2* mutants were established. For this purpose, calli were first produced from seeds. To confirm that the lines were genetically identical to parental plants (Tarantino et al., 2010), genomic DNA was purified from both *atfer4-1* and *atfer4-2* cells and the junctions of T-DNA insertions were amplified and sequenced. The results match those already published for *atfer4-1* and *atfer4-2* plants (Tarantino et al., 2010), i.e. T-DNA is inserted at position –57 (+1 is ATG start codon) of the *AtFer4* gene in the *atfer4-1* mutant and at position -61 in the *atfer4-2* mutant (not shown). In contrast to observations in *atfer4* KO plants (Ravet et al., 2009; Tarantino et al., 2010), however, a dramatically reduced but still detectable *AtFer4* transcript was present in both *atfer4* mutants when grown in suspension (Fig. 1A). Since the primers used for the RT-PCR reactions are specific for the *AtFer4* gene, these results suggest that the residual 57 bp/61 bp promoter sequences downstream of the insertions are enough to drive a residual *AtFer4* gene transcription, when cells are grown in this heterotrophic condition.

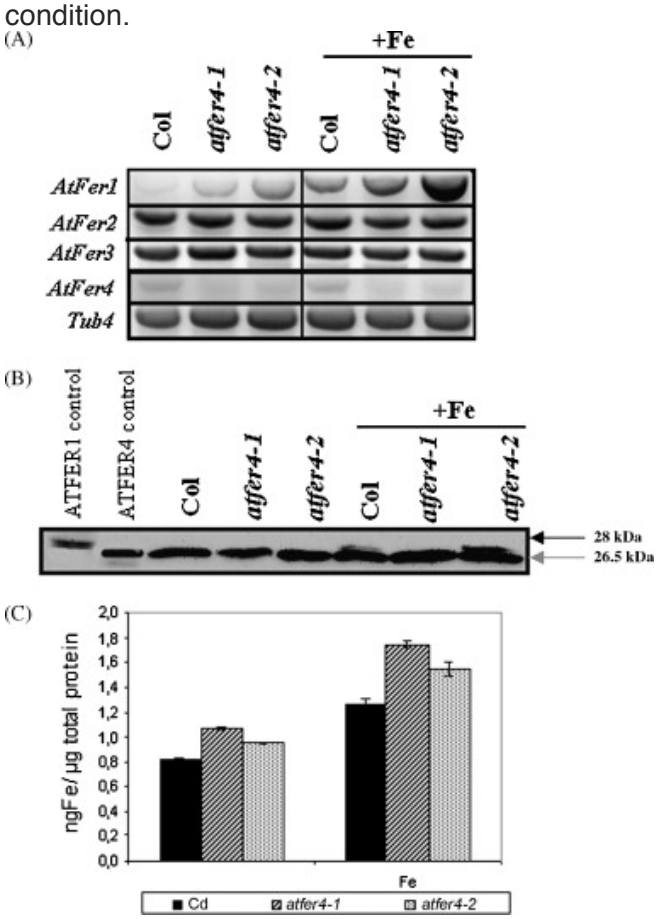

Download full-size image

Fig. 1. Cellular ferritin and Fe content. (A) RT-PCR analysis of *AtFer1-4* transcript levels in Col, *atfer4-1* and *atfer4-2* cells grown in control or '+Fe' condition. *Tub4* is the control, for equal addition

of RNA in each sample. (B) Protein gel blot analysis of ferritin content in Col, *atfer4-1* and *atfer4-2* cells grown in control or '+Fe' condition. 50 µg proteins were loaded in each lane, except ATFER1 control (25 µg) and ATFER4 control (100 µg). Filter was hybridized with the polyclonal antibody anti-Ferritin. (C) Total Fe content in Col, *atfer4-1* and *atfer4-2* cells grown in control or '+Fe' condition. Each bar indicates the mean value ± SE of 6 samples of 25 mg cells each.

AtFer1 transcript accumulation was observed in the '+Fe' condition, particularly in *atfer4* cells (Fig. 1A). Both *AtFer2* and *AtFer3* transcripts accumulated in wt as well as in *atfer4* mutant cells, in both the control and in the (+Fe) condition. These results are particularly surprising; the ATFER2 protein is the only ferritin isoform not present in *Arabidopsis* vegetative tissues, accumulating in seeds only (Ravet et al., 2009). Also, strong accumulation of the *AtFer3* transcript has been reported, until now, only under iron loading conditions (Petit et al., 2001) or under abiotic stresses (Tarantino et al., 2003).

Gel blot analysis of total protein extracts from Col, *atfer4-1* and *atfer4-2* cells collected after growth in control or '+Fe' conditions was performed. For this purpose, the following ATFER1 and ATFER4 positive controls were used: total protein extract from wt leaves collected after 24 h infiltration with 500 µM Fe (III)-citrate enriched in the 28 kDa ATFER1 (Briat et al., 2007, 2010) (Fig. 1B, ATFER1 control), and the mitochondrial protein extract from (+Fe) wt Col plants containing ATFER4 (Tarantino et al., 2010) (Fig. 1B, ATFER4 control). For blot hybridization, the polyclonal anti-Ferritin antibody, able to detect all the *Arabidopsis* ferritin isoforms (Murgia et al., 2007; Tarantino et al., 2010), was used. Total ferritin content was not reduced in *atfer4* cells when compared to wt counterparts, either in the control or in the '+Fe' condition (Fig. 1B). By contrast, a slight accumulation of total ferritin content was observed in all '+Fe' lines. These results were confirmed by using the anti-ATFER1 polyclonal antibody, also able to detect all the four *Arabidopsis* ferritins (Dellagi et al., 2005; Ravet et al., 2009) (Figure S1A). As additional controls, protein extracts from pea seeds, rich in ferritin (Murgia et al., 2007), or protein extracts from *atfer1* KO leaves lacking ATFER1 (Murgia et al., 2007), were also used (Figure S1B).

It is known that, in leaves, mature ATFER1 is 28 kDa MW, whereas mature ATFER4 and mature ATFER3 are 26.5 kDa MW (Ravet et al., 2009; Tarantino et al., 2010). The ferritin isoform accumulating in suspension cultured cells, in wt as well in *atfer4* ones, is also 26.5 kDa MW (Fig. 1B). These results cannot exclude the hypothesis that, in *atfer4* cells, ATFER4 levels are the same as wt ones regardless of the dramatically reduced *AtFer4* transcript levels. This hypothesis is, however, difficult to reconcile with the number of phenotypes observed in both *atfer4-1* and *atfer4-2* cells, as described below and discussed further in the Discussion. Regardless of the dramatic reduction of *atfer4* transcript presumably leading to a reduction in ATFER4 protein content, the overall ATFER1+ATFER2 + ATFER3 + ATFER4 content was not diminished in *atfer4* cells with respect to wt. Notably, *atfer4-1* and *atfer4-2* cells contained more total Fe than wt, in control as well as in '+Fe' conditions (Fig. 1C).

atfer4 cells show no reduction in mitochondrial ferritin content but an increase in mitochondrial Fe content

Mitochondria were purified by applying a protocol that relies on two different Percoll gradients (Sweetlove et al., 2006) (Figure S2) from wt, *atfer4-1* and *atfer4-2* cells grown either in control or '+Fe' conditions and were assayed for membrane integrity. Table S1 shows that almost 100% of both *atfer4-1* and *atfer4-2* mitochondria purified from cells grown in the control condition were undamaged. Conversely, integrity of mitochondria purified from '+Fe' cells was reduced in all lines, ranging from 53 to 64% (Table S1). Gel blot analysis of Col, *atfer4-1* and *atfer4-2* mitochondrial proteins purified from either control or '+Fe' cells showed that, in wt mitochondria, ferritins accumulated only under the '+Fe' condition, which is consistent with results from whole plants (Tarantino et al., 2010) (Fig. 2A). Also, *atfer4* mitochondria were devoid of ferritins under control conditions, with the exception of a band observed only in *atfer4-1* mitochondria (Fig. 2A, light grey arrow; see also Figure S1C), which was <26.5 kDa. As already described for total ferritin content in whole cells, the overall ATFER1 + ATFER2 + ATFER3 + ATFER4 content was not diminished in '+Fe' *atfer4* mitochondria with respect to wt. Indeed, a 26.5 kDa ferritin, particularly intense in

atfer4-1, was detected in all tested mitochondria (Fig. 2A; see also Figure S1C). Moreover, a <26.5 kDa band was also detected with the anti-Ferritin antibody only (Fig. 2A; see also Figure S1C). It should be noted that, to date, experimental evidence for mitochondrial localization has been provided for ATFER4 only (Tarantino et al., 2010). However, there is some evidence from *in vitro* dual-targeting experiments that the other isoforms might also be targeted, to some extent, to mitochondria (Sondermann and Klösgen, personal communication and unpublished results).

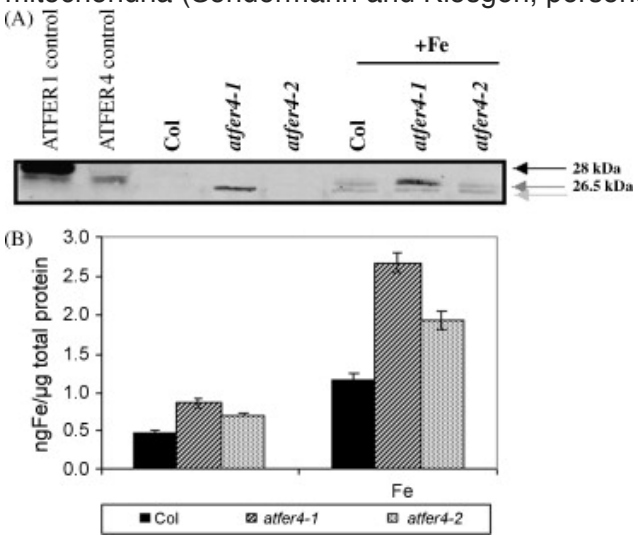

Download full-size image

Fig. 2. Mitochondrial ferritin and Fe content. (A) Protein gel blot analysis of ferritin content in Col, *atfer4-1* and *atfer4-2* mitochondria, purified from cells grown either in control or '+Fe' condition. 50 µg proteins were loaded in each lane (including ATFER4) with the exception of ATFER1 control (25 µg). Filter was hybridized with the polyclonal antibody anti-Ferritin. (B) Total iron content in Col, *atfer4-1* and *atfer4-2* mitochondria, purified from cells grown in control or '+Fe' condition. Each bar indicates the mean value ± SE of 3 samples consisting of 330 µg mitochondrial proteins each.

Similar to observations at the cellular level, total Fe content of *atfer4-1* and *atfer4-2* mitochondria was higher than levels in wt, in control as well as in '+Fe' conditions (Fig. 2B).

atfer4 cells show higher H2O2 content and higher cell death

When grown in suspension culture, *atfer4-1* and *atfer4-2* cells showed a darker appearance (Figure S3) and enhanced cell death (Fig. 3). Cellular parameters were altered in *atfer4-1* and *atfer4-2* mutants. Cells were indeed smaller in size (Fig. 4A), with smaller vacuoles (Fig. 4A) as confirmed by increased DW/FW ratios, DNA and protein contents (Table S2). An excess of H2O2 accumulated in *atfer4* cells and, in particular, close to plasma membranes, as shown by cell staining with DAB (Fig. 4B). Plasma membranes of *atfer4* cells grown in control conditions did not show, with TEM analysis, any structural alteration when compared to wt cells (Fig. 5A). '+Fe' *atfer4* cells appeared damaged, and plasmolysis was frequently observed in *atfer4* mutants (Fig. 5B, see also Figure S4), with plasma membranes partially retracted from cell wall. Such plasmolysis is not due to an artefact caused by the fixation procedure, since in this case, damage to mitochondria cristae, as well as to Golgi membranes would be also expected (Fig. 5). The alteration of plasma membranes in *atfer4* cells can be therefore genuinely correlated to alteration in *AtFer4* levels. The so-called 'handle-bar' mitochondria have been reported to be associated with Fe deficiency in cucumber roots (Vigani et al., 2009). They were, however, observed in wt cells grown in control conditions (Figure S5), indicating that they are not specifically related to Fe deficiency.

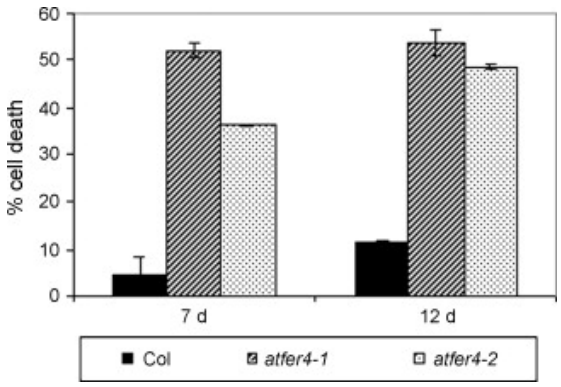

Download full-size image

Fig. 3. Cell viability in wt and *atfer4* cells. Cell death (%) in Col, *atfer4-1* and *atfer4-2* cells, grown for 7 or 12 d in control condition. Each bar indicates the mean value ± SE of 6 samples consisting of 0.3 g cells each.

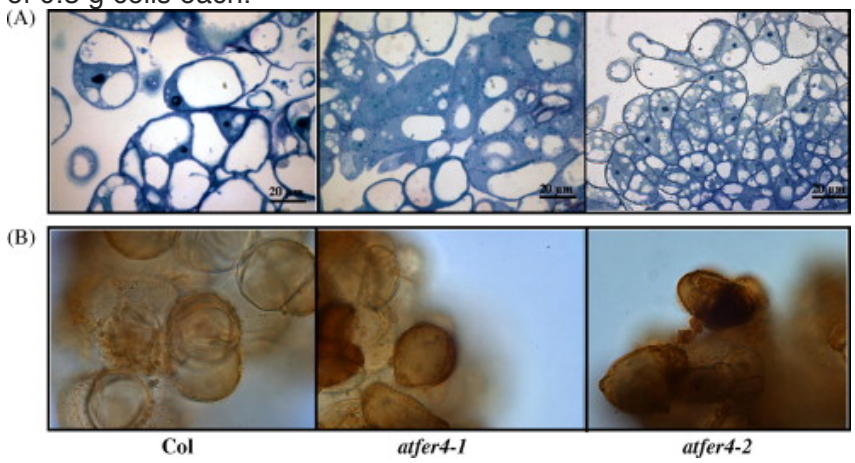

Download full-size image

Fig. 4. Morphology and ROS accumulation in wt and *atfer4* cells. (A) Light microscopy analysis of Col, *atfer4-1* and *atfer4-2* cells; bars correspond to 20 µm. (B) DAB staining of Col, *atfer4-1* and *atfer4-2* cells.

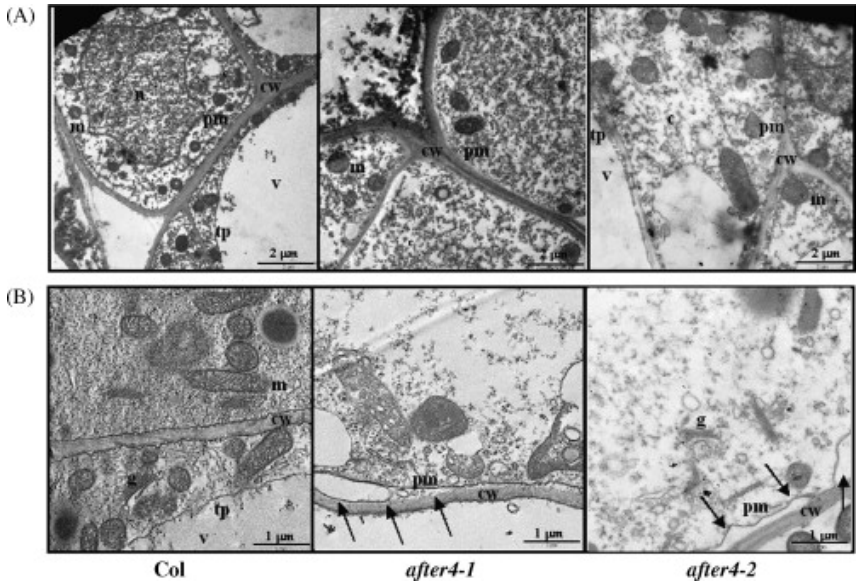

Download full-size image

Fig. 5. TEM analysis of wt and *atfer4* cells. TEM micrographs of Col, *atfer4-1* and *atfer4-2* cells grown in control (A) or '+Fe' condition (B). c: cytoplasm, cw: cell wall, g: golgi apparatus, m: mitochondria, n: nucleus, pm: plasma membrane, tp: tonoplast, v: vacuole. Scale bars: 2 µm (A),

1 µm (B). Partial plasmolysis in '+Fe' *atfer4-1* and *atfer4-2* cells (B) is indicated by arrows.

FRO3 transcript levels are higher in *atfer4* cells

Correlation analysis is a powerful tool to examine gene function and to identify candidate genes for specific processes (Menges et al., 2007, 2008). One of the simplest methods to perform the analysis involves the comparison of the transcript levels of a gene of interest against the transcript levels of any other genes in the genome and measuring the extent of correlation, such as the Pearson's correlation coefficient (Menges et al., 2008).

Correlation analysis of the 4 *Arabidopsis* ferritin isoforms, *AtFer1-4*, with either the ABC-like transporter *STA1*, putatively involved in Fe-efflux, the two Ferric reductase oxidases, *FRO3* and *FRO8*, putatively localized in the mitochondria, or the chloroplastic *FRO7* (Jeong and Connolly, 2009) showed that the highest correlation was between *AtFer4* and *FRO3*, with a Pearson's coefficient value of –0.441 in the linear analysis and –0.449 after log transformation (Table S3A and S3B, respectively). *FRO3* transcript accumulated in both *atfer4* cells (Fig. 6) much more than in wt cells grown under the same conditions in which, as expected, *FRO3* levels were very low (Fig. 6). Also, as expected, such high *FRO3* transcript levels were slightly reduced in '+Fe' *atfer4* cells, but still much higher than those observed in '+Fe' wt cells (Fig. 6). *FRO7*, *FRO8* and *STA1* transcripts levels did not change in *atfer4* cells when compared to wt cells, either in control or in (+Fe) conditions. The *FRO7* and *FRO8* genes were not expressed, whereas the *STA1* gene was highly expressed in all tested samples (Fig. 6).

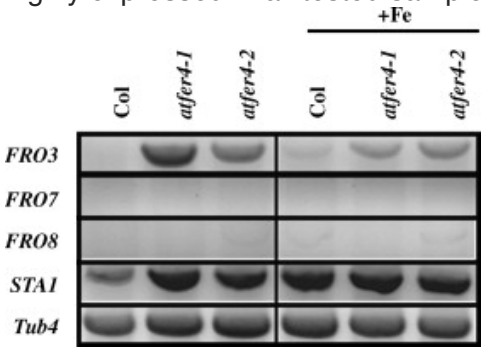

Download full-size image

Fig. 6. *FRO3*, *FRO7*, *FRO8*, *STA1* transcript levels in wt and *atfer4* cells. RT-PCR analysis of *FRO3*, *FRO7*, *FRO8*, *STA1* transcript levels in Col, *atfer4-1* and *atfer4-2* cells grown in control or '+Fe' condition. *Tub4* is the control, for equal addition of RNA in each sample.

O2 consumption rates are reduced in *atfer4* cells

The higher Fe content observed in mitochondria purified from both control and (+Fe) *atfer4* mutant cells (Fig. 2B) was associated with enrichment in the two mitochondrial [Fe-S] proteins Alternative Oxidase (AOX) and NAD9 (belonging to Complex I) (Fig. 7).

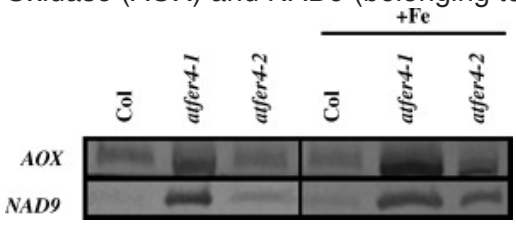

Download full-size image

Fig. 7. Protein gel blot analysis of AOX and NAD9 content in Col, *atfer4-1* and *atfer4-2* mitochondria, purified from cells grown either in control or '+Fe' condition. 50 µg proteins were loaded in each lane.

When grown under control conditions, however, *atfer4-1* and *atfer4-2* cells showed significantly lower O2 consumption rates than wt (Fig. 8A). Under Fe excess, O2 consumption rates increased in all tested lines with no differences among them (Fig. 8A). When control cells were treated with either KCN, which blocks the respiratory electron transfer chain, with SHAM, which blocks the Alternative Oxidase (Buchanan et al., 2000) or both of them, *atfer4-1* and *atfer4-2* O2 consumption

rates were still lower than those detected in wt cells (Fig. 8B).

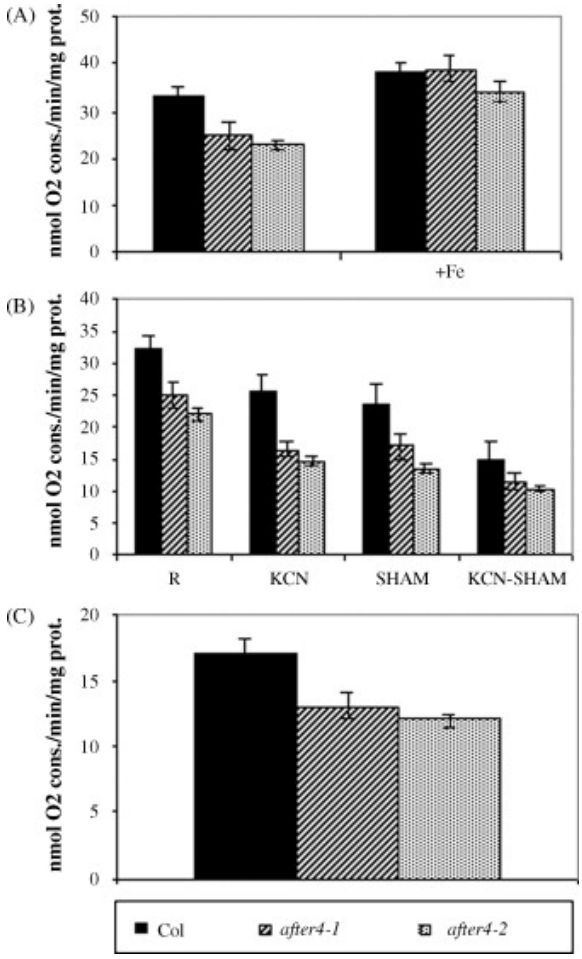

Download full-size image

Fig. 8. Total and respiration-dependent O2 consumption rates in wt and *atfer4* cells. (A) Total O2 consumption rates (nmol O2 consumed/min/mg total proteins) in cells grown in control or '+Fe' condition. (B) O2 consumption rates in cells grown in control conditions with addition of 10 mM KCN, or 2 mM SHAM or both. Total O2 consumption rates, indicated as initial values (IR, leftmost bars), are the same reported in (A). (C) Respiration-dependent O2 consumption rates, calculated by subtracting the O2 consumption values measured in the presence of KCN + SHAM (panel B) from the IR values. All measurements were made on 100 mg FW cells. Each bar is the mean value of 5 samples ± SE.

The respiration-dependent O2 consumption rates, obtained by subtracting the rates measured in the presence of KCN + SHAM (reflecting the O2 consumption not due to respiration) from the total O2 consumption (indicated as initial rate, IR), were still lower in *atfer4-1* and *atfer4-2* cells than in the wt cells (Fig. 8C).

Discussion

Mitochondrial Fe trafficking should satisfy organelles' demands for Fe without allowing its accumulation in dangerous, redox-active forms (Bowler et al., 1992). How regulation of intracellular, and in particular, of mitochondrial Fe compartmentalization and its dependence on organellar Fe-status occurs in plant cells is still not well understood. Unresolved key questions include: (i) Which organelle has the priority of Fe uptake under different conditions of external Fe availability? (ii) How is mitochondrial Fe status sensed? (iii) How does such Fe status integrate with the Fe demand in the other subcellular compartments?

The first evidence for the localization of plant ferritin in mitochondria (Zancani et al., 2004) was confirmed by the identification of *Arabidopsis* ATFER4 as the ferritin isoform targeted to mitochondria of *Arabidopsis* plants treated with constant Fe excess (Tarantino et al., 2010).

Proteome analysis of chloroplasts identified ATFER4 as a stromal-localized protein (Plant Proteome Database at http://ppdb.tc.cornell.edu). Thus, according to the nomenclature currently used (Peters and Small, 2001), ATFER4 can be properly described as 'dual targeted'. The goal of the present work was to unravel the physiological relevance of *AtFer4* when *Arabidopsis* cells are grown in heterotrophy. Such an approach offers not only technical advantages, such as the possibility to isolate pure mitochondria (which is not feasible when starting from *Arabidopsis* green tissues) but, most importantly, the reduction in complexity of the experimental model, since such cultures lack mature chloroplasts. For this reason, suspension cultures of *Arabidopsis* wt Col, as well as of *atfer4-1* and *atfer4-2* mutants were produced. Ferritin protein is detectable, in such cells, already under control conditions, in contrast to observations in maize (Savino et al., 1997) and soybean (Lescure et al., 1991), where ferritin accumulated only after Fe treatment. However, such Fe-dependent ferritin accumulation in maize and soybean cells was preceded by Fe starving, i.e. growth of cells in medium without Fe. Fe was present, though not in excess, in the control medium described in the present work, in order to guarantee optimal cell growth. A strong accumulation of *AtFer1* ferritin transcript upon treatment with Fe excess has been described in the past on *Arabidopsis* suspension cultures (Ler ecotype) (Murgia et al., 2002), whereas induction upon treatment with Fe excess was not very strong in the wt cells in the present study. We cannot exclude the possibility that the intensity of the response to Fe excess could be due to the metabolic adaptation of cells to growth in liquid. For that reason, it might be important that all the lines tested, including controls, are the same age and cultured under the same conditions (temperature, rpm), as we did in the present work.

Our results, while confirming that ferritin is present in *Arabidopsis* mitochondria under Fe excess, show that *atfer4* cells, even under control conditions with no excess Fe applied, manifest an altered phenotype. Specifically, these cells showed reduced cell and vacuole size, damage of plasma membranes, higher H2O2 accumulation, higher cell death, reduction of O2 consumption rates, higher cellular as well as mitochondrial Fe content, and also higher AOX and NAD9 content. The lack of reduction of total ferritin content in *atfer4* cells and in '+Fe' *atfer4* mitochondria compared to wt, could suggest that ATFER4 protein synthesis remains unaltered in *atfer4* cells, due to the presence of residual *AtFer4* transcription, in contrast to previous observations in *atfer4* plants (Tarantino et al., 2010). However, the various phenotypes described in the present work for both *atfer4* mutants would not support such possibility hypothesis. Moreover, the higher cellular and mitochondrial Fe content observed in both *atfer4* mutants strongly supports the hypothesis that the observed phenotypes are due to a specific alteration in the Fe trafficking.

The lack of marked alteration of total ferritin content in *atfer4* cells, as well as in *atfer4* mitochondria, compared to wt cells, would indeed suggest that the complex molecular network keeping Fe cellular homeostasis under control is partially controlled by *AtFer4* transcript and/or that a precise ratio of the various ferritin protein isoforms is required.

The lack of ATFER4 must be compensated by an increase in at least one of the other three ferritin isoforms. The evidence that *AtFer1* transcript is increased in *atfer4* cells would suggest its involvement in such compensation. This hypothesis would, however, imply further ATFER1processing from 28 kDa to 26.5 kDa in heterotrophic cells, which does not occur in mature green leaves (Ravet et al., 2009). On the other hand, ferritin regulation observed in the *Arabidopsis* cells cultures differs from that observed in plant tissues, as the reported accumulation of *AtFer2* and *AtFer3* transcripts, described in the present work, testifies. In conclusion, each of the ATFER1/ATFER2/ATFER2 isoforms might be compensating for the lack of ATFER4.

How the knocking-out of the single isoform *AtFer4* can be responsible for all the observed effects is puzzling. There are indications that mammalian ferritin might also act as a signaling molecule (Recalcati et al., 2008; Arosio et al., 2009) and not just an Fe-store.

Correlation analysis has the potential to assign a gene to a particular gene network, and it is therefore complementary to microarray analysis. Such an analysis predicted the involvement of *AtFer4* and *FRO3* genes in the same network controlling intracellular iron homeostasis and for which *AtFer4* gene is a determinant. The experimental approach confirmed that *FRO3* is the only

gene, among the tested FROs, whose transcription is altered in *atfer4* cells.
FRO3 transcript levels were very high in *atfer4* cells grown under control conditions, in which mitochondria have higher mitochondrial Fe content than wt. It is also known that *FRO3* accumulates upon Fe deficiency (Mukherjee et al., 2006; Jeong and Connolly, 2009), so the 'sensing mechanism' of Fe-status triggering *FRO3* accumulation seems to be partially dependent on extra-mitochondrial Fe status, since it triggers signal(s) of Fe deficiency-like status in *atfer4* cells possessing higher mitochondrial Fe content. This hypothesis is supported by the finding that *FRO3* levels are slightly reduced in '+Fe' *atfer4* cells (though still much higher when compared to '+Fe' wt cell), whereas their mitochondrial Fe content increases further. The higher Fe content observed in *atfer4* mitochondria is associated with higher content of two Fe-containing mitochondrial proteins: NAD9, involved in the respiratory electron transfer chain, as well as AOX, involved in the mitochondrial energy dissipating system. Such an increase in proteins involved in mitochondrial electron flow, however, does not cause a higher respiratory O2 consumption rate in *atfer4* cells grown in control conditions. On the contrary, the consumption rate is diminished. These results suggest that the electron transfer chain of *atfer4* mitochondria is partially damaged due to the Fe overload and consequent oxidative damage. All the phenotypes described for *atfer4* cells in the present work support such hypothesis.
atfer4-1 is, between the two allelic mutants analyzed, the one with strongest phenotypes. It will interesting, in the future, to address the question of what makes the *atfer4-1* mutant allele stronger than the *atfer4-2* allele, as that their T-DNA insertions are only 4 bases apart in the *AtFer4* gene promoter. In any case, all the phenotypes described for *atfer4* cells are consistent with the proposal that the observed higher Fe accumulation in *atfer4* mitochondria, as well as the higher ROS levels and increased cell death, are all consequences of improper cytosolic Fe homeostasis and trafficking.
A challenging question is why such a role did not emerge in the analysis of *atfer4* plants (Tarantino et al., 2010). A possible explanation is that the heterotrophic cultivation in which photosynthesis is not active would recreate a milieu partially resembling the early host cell in which the endosymbiosis of cyanobacteria did not yet occur (Kutschera and Niklas, 2005). It is therefore possible that the regulatory role of *AtFer4* described in the present work is an ancestral one, almost, even though not completely lost, during the evolution of green plants.
Acknowledgements
We thank Valentina Vazzola for help during the cultivation of mutant lines, Ralf Berndt Klösgen and coworkers for communicating unpublished data, Marcello Iriti for the DAB staining and Nicoletta Beffagna for allowing access to all her laboratory equipment, help during mitochondria purification and for her manuscript revision. Janneke Balk kindly donated NAD9 and AOX antibodies to Gianpiero Vigani. We are grateful to Jean Francois Briat and to Frederic Gaymard for the anti-ATFER1 polyclonal antibody and for their valuable comments on the manuscript. This work was supported by MIUR [PRIN 2006, prot. Nr. 2006058818 and PRIN 2008, prot. Nr. 20084XTFBC]. D. Tarantino was partially supported by INGENIO grants.
Appendix A. Supplementary data

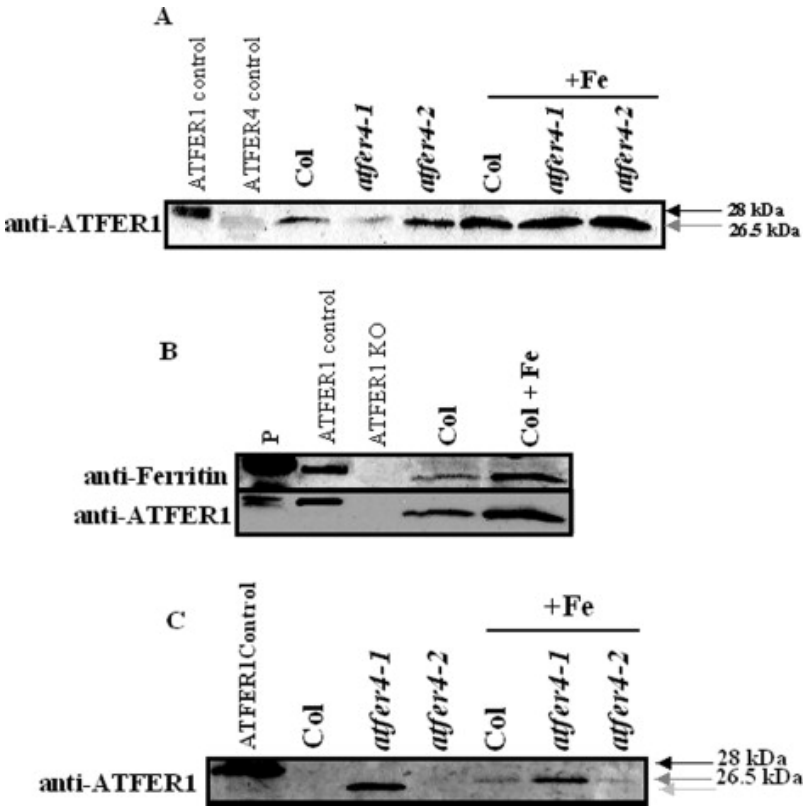

Download full-size image

Supplementary Figure S1. Ferritin content in whole cells and mitochondria. (A) Protein gel blot analysis of ferritin content in Col, *atfer4-1* or *atfer4-2* cells, in control or '+Fe' condition. ATFER1 control: 25 µg crude protein extract from wt Col leaves collected after 24 h infiltration with 500 µM Fe (III)-citrate; ATFER4 control: 100 µg proteins from mitochondria purified from Col plants constantly irrigated with 2.15 mM Fe supplement; 50 µg proteins were loaded in all other lanes. Filters were hybridized with the polyclonal antibody anti-ATFER1. (B) Protein gel blot analysis of same Col samples as described in (A) with the following further controls: 10 µg pea seeds protein extract (indicated as P) and 25 µg protein extracts from *atfer1* KO leaves (ATFER1 KO). Filter was hybridized with either polyclonal antibody anti-Ferritin or with anti-ATFER1. (C) Protein gel blot analysis of ferritin content in Col, *atfer4-1* and *atfer4-2* mitochondria, purified from cells grown either in control or '+Fe' condition; 50 µg proteins were loaded in each lane. ATFER1 control as in (A). Filter was hybridized with anti-ATFER1 polyclonal antibody.

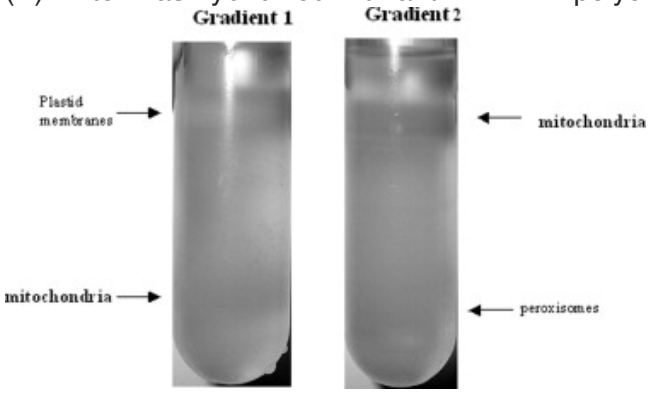

Download full-size image

Supplementary Figure S2. Mitochodria purification from Percoll gradients. The two Percoll gradients of a typical mitochondria purification, are shown. In gradient 1, the bands consisting either of plastid membranes or mitochondria are shown. In gradient 2, bands consisting of either mitochondria or peroxisomes are shown.

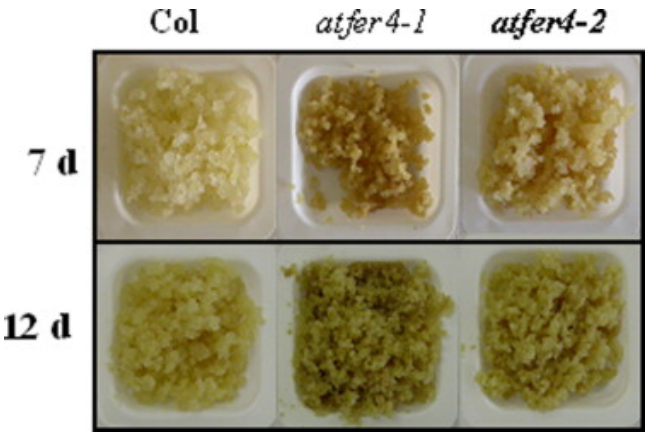

Download full-size image

Supplementary Figure S3. Phenotype of Col and *atfer4* cell cultures. Appearance of 7 or 12 d Col, *atfer4-1* and *atfer4-2* suspension cultured cells, after filtration.

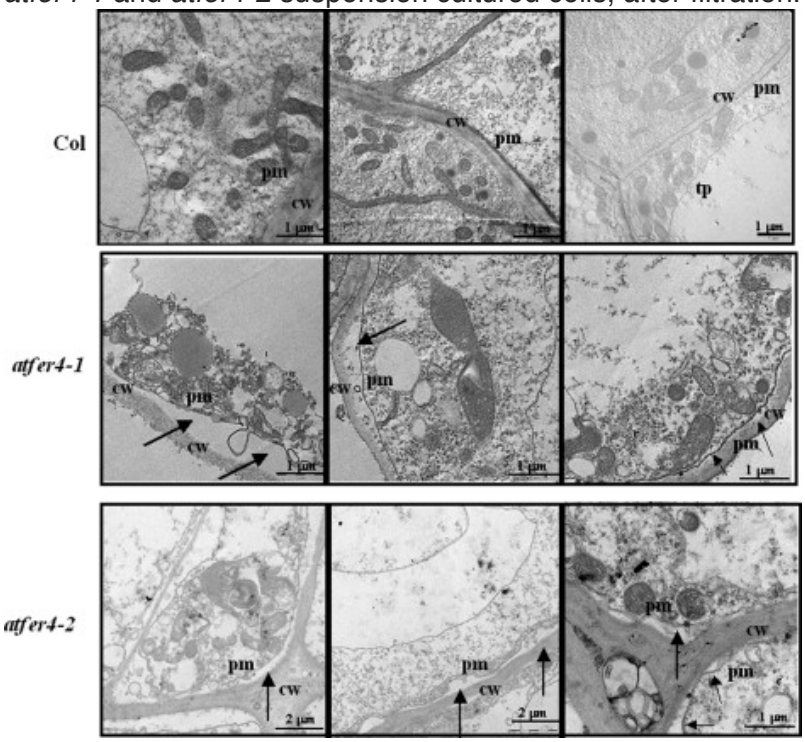

Download full-size image

Supplementary Figure S4. TEM analysis of '+Fe' wt and *atfer4* cells. TEM micrographs of Col, *atfer4-1* and *atfer4-2* cells in '+Fe' condition: for each line three different micrographs are reported. cw: cell wall, pm: plasma membrane. Scale bars: either 2 µm or 1 µm, as indicated in each picture. Retraction of plasma membrane from cell wall, in '+Fe' *atfer4-1* and *atfer4-2* cells, is indicated by arrows.

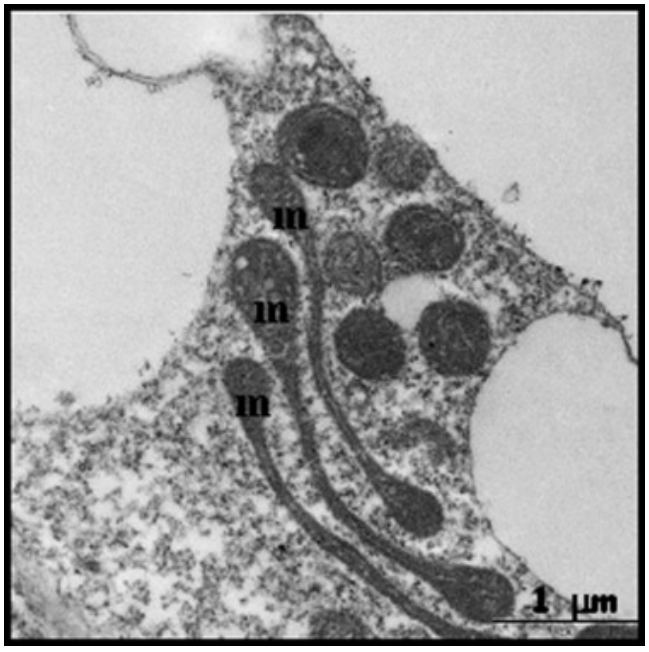

Download full-size image

Supplementary Figure S5. Handle-bar mitochondria in Col cells. TEM micrograph of Col suspension cultured cells grown in control condition; m: mitochondria with handle-bar shape. Scale bar: 1 µm.

			+Fe		
Col	*atfer4-1*	*atfer4-2*	Col	*atfer4-1*	*atfer4-2*
78 ± 6	100 ± 3	100 ± 1	64 ± 6	55 ± 2	53 ± 2

Download full-size image

Supplementary Table S1. Integrity of purified mitochondria. Integrity (percent value) of mitochondria purified from Col, *atfer4-1* and *atfer4-2* cells, grown in control or '+Fe' condition, evaluated through the cytochrome-c oxidase assay (see Materials and methods). Each value represents the mean value of at least 4 measurements ± SE.

				+ Fe		
	Col	*atfer4-1*	*atfer4-2*	Col	*atfer4-1*	*atfer4-2*
FW (g)	1	1	1	1	1	1
DW (mg)	40 ± 2	52 ± 1	59 ± 2	38 ± 1	77 ± 3	56 ± 2
Proteins (mg)	5.3 ± 0.3	20.2 ± 1	14.5 ± 0.5	3.2 ± 0.8	15.2 ± 0.9	9.9 ± 0.7
total DNA (mg)	1.96 ±0.08	5.27 ±0.14	6.80 ±0.17			

Download full-size image

Supplementary Table S2. Water, DNA and protein content in Col and in *atfer4* suspension cultures. Col, *atfer4-1* and *atfer4-2* cells grown in control or '+Fe' condition were filtered, weighed and divided into 1 g FW aliquots; DW (mg), protein (mg) and total DNA content (mg) of each aliquot was quantified. Reported values are mean values of at least 6 independent samples ± SE.

A

	STA1	FRO3	FRO7	FRO8	AtFer1	AtFer2	AtFer3	AtFer4
STA1 (At5g58270)	1	-0.174	0.316	0.136	0.001	0.363	0.165	0.068
FRO3 (At1g23020)	-0.174	1	0.027	-0.068	-0.233	-0.151	-0.286	**-0.441**
FRO7 (At5g49740)	0.316	0.027	1	0.396	0.171	-0.126	-0.127	0.020
FRO8 (At5g50160)	0.136	-0.068	0.396	1	0.060	-0,150	-0.212	0.009
AtFer1 (At5g01600)	0.001	-0.233	0.171	0.060	1	-0.110	0.253	0.284
AtFer2 (At3g11050)	0.363	-0.151	-0.126	-0.150	-0.110	1	-0.123	-0.100
AtFer3 (At3g56090)	0.165	-0.286	-0.127	-0.212	0.253	-0.123	1	0.443
AtFer4 (At2g40300)	0.068	**-0.441**	0.020	0.009	0.284	-0.100	0.443	1

B

	STA1	FRO3	FRO7	FRO8	AtFer1	AtFer2	AtFer3	AtFer4
STA1 (At5g58270)	1	-0.190	0.365	0.220	-0.050	0.156	0.176	0.131
FRO3 (At1g23020)	-0.190	1	0.073	0.012	-0.144	-0.185	-0.267	**-0.449**
FRO7 (At5g49740)	0.365	0.073	1	0.696	0.048	-0.402	-0.047	0.304
FRO8 (At5g50160)	0.220	0.012	0.696	1	0.012	-0.588	-0.199	0.214
AtFer1 (At5g01600)	-0.050	-0.144	0.048	0.012	1	-0.008	0.378	0.399
AtFer2 (At3g11050)	0.156	-0.185	-0.402	-0.588	-0.008	1	0.089	-0.119
AtFer3 (At3g56090)	0.176	-0.267	-0.047	-0.199	0.378	0.089	1	0.524
AtFer4 (At2g40300)	0.131	**-0.449**	0.304	0.214	0.399	-0.119	0.524	1

Download full-size image

Supplementary Table S3. Pearson's correlation coefficients of pairwise comparison of gene expression levels. For each table the list of analysed genes and their corresponding AGI codes are reported. (A) Pearson's coefficients calculated on expression values. (B) Pearson's coefficients calculated on values after log transformation. The values for the *FRO3–AtFer4* pair are highlighted in bold.

References

Arosio et al., 2009
P. Arosio, R. Ingrassia, P. Cavadini
Ferritins: a family of molecules for iron storage, antioxidation and more
Biochim Biophys Acta, 1790 (2009), pp. 589-599
ArticlePDF (626KB)View Record in Scopus

Bowler et al., 1992
C. Bowler, M. van Montagu, D. Inzè
Superoxide dismutase an stress tolerance
Annu Rev Plant Physiol Plant Mol Biol, 43 (1992), pp. 83-116
CrossRefView Record in Scopus

Briat et al., 2007
J.F. Briat, C. Curie, F. Gaymard
Iron utilization and metabolism in plants
Curr Opin Plant Biol, 10 (2007), pp. 276-282
ArticlePDF (752KB)View Record in Scopus

Briat et al., 2010
J.F. Briat, N. Arnaud, C. Duc, J. Boucherez, B. Touraine, F. Cellier, *et al.*
New insights into ferritin synthesis and function highlight a link between iron homeostasis and oxidative stress in plants
Ann Bot (2010), 10.1093/aob/mcp128

Buchanan et al., 2000
B.B. Buchanan, W. Gruissem, R.L. Jones
Biochemistry and molecular biology of plants
American Soc Plant Physiologists (2000)

ISNB 0-943088-39-9

Campanella et al., 2004
A. Campanella, G. Isaya, H. O'Neill, P. Santambrogio, A. Cozzi, P. Arosio, *et al.*
The expression of human mitochondrial ferritin rescues respiratory function in frataxin-deficient yeast
Hum Mol Genet, 13 (2004), pp. 2279-2288
CrossRefView Record in Scopus
Campanella et al., 2009
A. Campanella, E. Rovelli, P. Santambrogio, A. Cozzi, F. Taroni, S. Levi
Mitochondrial ferritin limits oxidative damage regulating mitochondrial iron availability: hypothesis for a protective role in Friedreich ataxia
Hum Mol Genet, 18 (2009), pp. 1-11
View Record in Scopus
Dellagi et al., 2005
A. Dellagi, M. Rigault, D. Segond, C. Roux, Y. Kraepiel, F. Cellier, *et al.*
Siderophore-mediated upregulation of *Arabidopsis* ferritin expression in response to *Erwinia chrysanthemi* infection
Plant J, 43 (2005), pp. 262-272
CrossRefView Record in Scopus
Guerinot and Yi, 1994
M.L. Guerinot, Y. Yi
Iron: nutritious, noxious and not ready available
Plant Physiol, 104 (1994), pp. 815-820
CrossRefView Record in Scopus
Hsiao and Bornman, 1989
K.C. Hsiao, C.H. Bornman
Cyanide-initiated oxygen consumption in autoclaved culture medium containing sugars
Plant Cell Rep, 8 (1989), pp. 90-92
CrossRefView Record in Scopus
Jeong and Connolly, 2009
J. Jeong, E.L. Connolly
Iron uptake mechanisms in plants: functions of the FRO family of ferric reductases
Plant Sci, 176 (2009), pp. 709-714
ArticlePDF (189KB)CrossRefView Record in Scopus
Jeong and Guerinot, 2009
J. Jeong, M.L. Guerinot
Homing in on iron homeostasis in plants
Trends Plant Sci, 14 (2009), pp. 280-285
ArticlePDF (217KB)View Record in Scopus
Kushnir et al., 2001
S. Kushnir, E. Babiychuk, S. Storozhenko, M. Davey, J. Papenbrock, R. De Ricke, *et al.*
A mutation of the mitochondrial ABC transporter Sta1 leads to dwarfism and chlorosis in the *Arabidopsis* mutant starik
Plant Cell, 13 (2001), pp. 89-100
CrossRefView Record in Scopus
Kutschera and Niklas, 2005
U. Kutschera, K.J. Niklas
Endosymbiosis, cell evolution and speciation
Theory Biosci, 124 (2005), pp. 1-24
ArticlePDF (830KB)CrossRefView Record in Scopus
Lescure et al., 1991

A.M. Lescure, D. Proudhon, H. Pesey, M. Ragland, E. Theil, J.F. Briat
Ferritin gene transcription is regulated by iron in soybean cell cultures
Proc Natl Acad Sci USA, 88 (1991), pp. 8222-8226
CrossRefView Record in Scopus
Levi and Rovida, 2009
S. Levi, E. Rovida
The role of iron in mitochondrial function
Biochim Biophys Acta, 1790 (2009), pp. 629-636
ArticlePDF (391KB)View Record in Scopus
Levi et al., 2001
S. Levi, B. Corsi, M. Bosisio, R. Invernizzi, A. Volz, D. Sanford, *et al.*
A human mitochondrial ferritin encoded by an intronless gene
J Biol Chem, 276 (2001), pp. 24437-24440
CrossRefView Record in Scopus
Mackenzie et al., 2008
E.L. Mackenzie, K. Iwasaki, Y. Tsuji
Intracellular iron transport and storage: from molecular mechanisms to health implications
Antiox Redox Signal, 10 (2008), pp. 997-1030
CrossRefView Record in Scopus
Menges et al., 2007
M. Menges, G. Pavesi, P. Morandini, L. Bögre, J.A. Murray
Genomic organization and evolutionary conservation of plant D-type cyclins
Plant Physiol, 145 (2007), pp. 1558-1576
CrossRefView Record in Scopus
Menges et al., 2008
M. Menges, R. Dóczi, L. Okrész, P. Morandini, L. Mizzi, M. Soloviev, *et al.*
Comprehensive gene expression atlas for the *Arabidopsis* MAP kinase signalling pathways
New Phytol, 179 (2008), pp. 643-662
CrossRefView Record in Scopus
Mukherjee et al., 2006
I. Mukherjee, N.H. Campbell, J.S. Ash, E.L. Connolly
Expression profiling of the *Arabidopsis* ferric chelate reductase (FRO) gene family reveals differential regulation by iron and copper
Planta, 223 (2006), pp. 1178-1190
CrossRefView Record in Scopus
Murgia et al., 2002
I. Murgia, M. Delledonne, C. Soave
Nitric oxide mediates iron-induced ferritin accumulation in *Arabidopsis*
Plant J, 30 (2002), pp. 521-528
CrossRefView Record in Scopus
Murgia et al., 2007
I. Murgia, V. Vazzola, D. Tarantino, F. Cellier, K. Ravet, J.F. Briat, *et al.*
Knock-out of the ferritin *AtFer1* causes earlier onset of age-dependent leaf senescence in *Arabidopsis*
Plant Physiol Biochem, 45 (2007), pp. 898-907
ArticlePDF (2MB)View Record in Scopus
Murgia et al., 2009
I. Murgia, D. Tarantino, C. Soave
Mitochondrial iron metabolism in plants: frataxin comes into play
Plant Soil, 325 (2009), pp. 5-14
CrossRefView Record in Scopus
Peters and Small, 2001

N. Peters, I. Small
Dual targeting to mitochondria and chloroplasts
Biochim Biophys Acta, 1541 (2001), pp. 22478-22482

Petit et al., 2001
J.M. Petit, J.F. Briat, S. Lobreaux
Structure and differential expression of the four members of the *Arabidopsis thaliana* ferritin gene family
Biochem J, 359 (2001), pp. 575-582
CrossRefView Record in Scopus
Ravet et al., 2009
K. Ravet, B. Touraine, J. Boucherez, J.F. Briat, F. Gaymard, F. Cellier
Ferritins control interaction between iron homeostasis and oxidative stress in *Arabidopsis*
Plant J, 57 (2009), pp. 400-412
CrossRefView Record in Scopus
Recalcati et al., 2008
S. Recalcati, P. Invernizzi, P. Arosio, G. Cairo
New functions for an iron storage protein: the role of ferritin in immunity and autoimmunity
J Autoimmun, 30 (2008), pp. 84-89
ArticlePDF (186KB)View Record in Scopus
Santambrogio et al., 2007
P. Santambrogio, G. Biasiotto, F. Sanvito, S. Olivieri, P. Arosio, S. Levi
Mitochondrial ferritin expression in adult mouse tissues
J Histochem Cytochem, 55 (2007), pp. 1129-1137
CrossRefView Record in Scopus
Savino et al., 1997
G. Savino, J.F. Briat, S. Lobreaux
Inhibition of the iron-induced ZmFer1 maize ferritin gene expression by antioxidants and serine/threonine phosphatase inhibitors
J Biol Chem, 272 (1997), pp. 33319-33326
CrossRefView Record in Scopus
Sweetlove et al., 2006
L.J. Sweetlove, N.L. Taylor, C.J. Leaver
Isolation of intact, functional mitochondria from the model plant *Arabidopsis thaliana*
Methods Mol Biol, 372 (2006), pp. 125-136

Tarantino et al., 2003
D. Tarantino, J.M. Petit, S. Lobreaux, J.F. Briat, C. Soave, I. Murgia
Differential involvement of the IDRS cis-element in the developmental and environmental regulation of the *AtFer4* ferritin gene from *Arabidopsis*
Planta, 217 (2003), pp. 709-716
CrossRefView Record in Scopus
Tarantino et al., 2010
D. Tarantino, F. Casagrande, C. Soave, I. Murgia
Knocking out of the mitochondrial *AtFer4* ferritin does not alter response of *Arabidopsis* plants to abiotic stresses
J Plant Physiol, 167 (2010), pp. 453-460
ArticlePDF (488KB)View Record in Scopus
Vazzola et al., 2007
V. Vazzola, A. Losa, C. Soave, I. Murgia
Knockout of frataxin causes embryo lethality in *Arabidopsis*
FEBS Lett, 581 (2007), pp. 667-672

Vigani et al., 2009
G. Vigani, D. Maffi, G. Zocchi
Iron availability affects the function of mitochondria in cucumber roots
New Phytol, 182 (2009), pp. 127-136
CrossRefView Record in Scopus
Zancani et al., 2004
M. Zancani, M. Peresson, A. Biroccio, G. Federici, A. Urbani, I. Murgia, *et al.*
Evidence for the presence of ferritin in plant mitochondria
Eur J Biochem, 271 (2004), pp. 3657-3664
CrossRefView Record in Scopus